https://doi.org/10.31436/iiumecp.v1i1.4443

SCREENING OF FABRICATION PARAMETERS FOR A LOW-COST MOLECULARLY IMPRINTED POLYMER (MIP)-BASED SENSOR FOR SULFAMETHOXAZOLE DETECTION

MUHAMMAD AZRI RAFIQ MOHD RASYIDI [1], AMANATUZZAKIAH ABDUL HALIM [1*], ROSMINAZUIN AB. RAHIM [2] AND ALIZA 'AINI MD RALIB [2]

[1]*Department of Chemical Engineering and Sustainability, Kulliyyah of Engineering, International Islamic University. Malaysia (IIUM), Jalan Gombak, 53100 Kuala Lumpur, Malaysia*
[2]*Department of Electrical & Computer Engineering, Kulliyyah of Engineering, International Islamic University. Malaysia (IIUM), Jalan Gombak, 53100 Kuala Lumpur, Malaysia*

**Corresponding author: amana@iium.edu.my*

ABSTRACT: The presence of sulfamethoxazole (SMX) residues in dairy products poses serious public health concerns, necessitating the development of low-cost and field-deployable screening instruments. While molecularly imprinted polymer (MIP)-based electrochemical sensors have shown promise selectivity for antibiotic detection, little attention has been paid to the screening of fabrication factors that have a significant impact on sensor performance. As a result, this research focuses on the screening of the critical fabrication parameters for a low-cost MIP-modified screen-printed carbon electrode (MIP/SPCE) platform for SMX detection. Cyclic voltammetry was used to assess the impact of carbon ink type (water-based versus solvent-based), stencil type (mesh stencil versus plotter cutter stencil), and MIP deposition volume (5 µL and 10 µL) on the electrochemical performance of the sensor. The MIP was synthesized by bulk polymerization and analyzed with scanning electron microscopy (SEM), which confirmed the successful creation of SMX-specific binding sites. Electrochemical screening findings showed that solvent-based carbon ink and plotter cutter stencils produced SPCEs with lower resistance (200-400 Ω) and well-defined redox peaks than their equivalents. Furthermore, a 5 µL MIP deposition volume exhibited optimum electron transport properties, providing a larger anodic peak current than thicker MIP layers. These findings emphasize the importance of fabrication parameter selection in obtaining consistent and sensitive MIP/SPCE performance. The improved manufacturing structure provides a solid platform for the future development of low-cost electrochemical sensors designed for routine antibiotic residue detection in food safety applications.

KEYWORDS: *Sulfamethoxazole (SMX), Molecular Imprinted Polymer (MIP), Screen Printed Carbon Electrode (SPE)*

1. INTRODUCTION

The presence of antibiotic residues in food products, particularly milk, has emerged as a critical public health concern. Sulfamethoxazole (SMX), one of the most widely applied sulfonamides in veterinary practice for the treatment of bacterial infections, is one of the most common antibiotics found in dairy products [1-6]. The presence of SMX residuals in the food chain presents health hazards such as allergic reactions and the rise of antibiotic-resistant bacterial communities. To prevent these possible health dangers, regulatory agencies have put in place a maximum residue limit (MRL) for SMX at 100 µg / kg (0.4 µM) [2][5]. Nonetheless,

https://doi.org/10.31436/iiumecp.v1i1.4443

conventional detection methods such as high-performance liquid chromatography (HPLC), mass spectrometry (MS), and enzyme-linked immunosorbent assay (ELISA) tend to incur high expenses, consume considerable time for completion, and need controlled laboratory settings, hence making them impractical for field or routine applications [1][3].

Electrochemical sensors have emerged as promising alternatives for antibiotic residue detection because of their mobility, quick reaction time, and cheap operational cost. Screen-printed electrodes (SPEs) have gained popularity due to their disposability, scalability, and compatibility with miniaturized sensing systems [7]. Despite these benefits, the electrochemical performance of SPEs is heavily influenced by production factors such as ink composition, printing process, and substrate material [8]. Previous research has shown that differences in carbon ink composition may have a considerable impact on electrode conductivity, surface roughness, and electron transfer kinetics, all of which affect sensor sensitivity and repeatability. Solvent-based carbon inks, for example, have been shown to have better conductivity and adhesion than water-based inks, particularly when higher curing temperatures are used [7][9].

In addition to ink composition, stencil manufacture procedures influence the quality of printed electrodes. Mesh stencils are widely employed in commercial screen-printing methods, however problems with mesh clogging, ink residue contamination, and irregular ink transfer have been documented, particularly in laboratory-scale manufacturing [9]. Alternatively, plotter cutter stencils made of polymeric sheets provide better pattern definition and cleaning, which may result in increased electrical continuity and decreased electrode resistance [9-10].

To improve selectivity for particular analytes like SMX, MIPs have been widely incorporated into electrochemical sensing devices. MIPs provide synthetic recognition sites that complement the target molecule's size, shape, and functional groups [11]. While much research has concentrated on enhancing MIP composition and binding affinity, few have investigated the effect of MIP deposition parameters, notably film thickness and loading volume, on electron transfer behavior. Excessive MIP layers can reduce redox probe diffusion and increase charge transfer resistance, whereas inadequate coverage can lead to poor selectivity and signal instability [11-12].

As a result, there is a significant research gap in the comprehensive evaluation of SPE manufacturing parameters and MIP deposition conditions for antibiotic detection sensors. Addressing this gap is critical for ensuring predictable performance, cheap production costs, and practical application of MIP-based electrochemical sensors in food safety monitoring. This work evaluates the effects of ink type, stencil fabrication, and MIP deposition volume on the performance of a MIP/SPCE sensor for SMX screening.

2. METHODOLOGY

2.1 Materials

Methacrylic acid (MAA), sulfamethoxazole (SMX), Ethylene glycol dimethacrylate (EGDMA), Azobisisobutyronitrile (AIBN), acetonitrile, methanol, acetic acid, ultrapure water, nitrogen gas, oil bath, Carbon ink, Silver chloride rod, potassium ferricyanide, thinner (toluene), ethanol, PBS (Sodium Chloride, Sodium Phosphate Dibasic (Na_2HPO_4), Potassium Chloride, Potassium Phosphate Monobasic ($KHPO_4$), distilled water).

https://doi.org/10.31436/iiumecp.v1i1.4443

2.2 The synthesis of MIP and NIP polymers

MIP using SMX as a template was prepared from a reagent mixture in a 10 ml glass vial obtained by mixing 5 mmol of the functional monomer methacrylic acid, 0.5 mmol of the cross linker EGDMA, 0.085 mmol of the template/target analyte SMX and 1.1 mmol of the initiator AIBN in 0.7 ml acetonitrile. The MIP mixture was uniformly dispersed in an ultrasound bath for 5 min. Then, it was stirred in an oil bath maintain at 60 °C for 20 h. The obtained solid polymer undergone washing with methanol several times for the removal of other materials from the polymer (e.g., residual monomers or oligomers and initiator fragments). The purity was confirmed optically by UV–vis spectrophotometry at 285 nm until no further residues detected. The template was extract by washing the MIP in a methanol/acetic acid solution (10:1, v/v) four times, each time for 10 min, and then twice in UPW for 10 min. The extraction of SMX was confirmed by UV–vis spectrophotometry at 285 nm until no traces of SMX were captured. The specific sorption of the analyte occured as a result of the formation of the cavities following the analyte extraction process. Finally, the MIP was dry to a constant weight in the oven at 60 °C. The non-imprinted polymer (NIP) was prepared by following a similar procedure as the MIP but without the SMX from the formulation, thus, no template removal step required. Finally, physical characterization was performed using Scanning Electron Microscopy (SEM).

2.3 Development of stencil

The process begins with designing SPE patterns using SolidWork software. According to Gamry Instruments, SPE was fabricated with dimensions of 25.40 mm in length, 7.26 mm in width, and 0.63 mm in thickness. The working electrode had a diameter of 2 mm, while the auxiliary electrode spans an area of 4.00 ± 0.05 mm². The SPE drawing was sent to the manufacturer to produce the stencil. The customized screen-printing meshes produced using photomask films by Khai Lien Silk Screen Suppliers. Then, another stencil was developed with self-made stencil used plotter cutter machine (Silhouette V4).

2.4 Printing of the SPE using ink

The stencil was flip horizontally before use to ensure proper alignment during the printing process. The PET substrate (0.3 mm thick) then placed under the flipped mesh, ready to receive the printed patterns. By using squeegee, carbon ink was printed to form the counter electrode and working electrode and dried and cured at 80°C for 10 minutes and 140°C for 45 minutes respectively. The printed SPE was characterized using cyclic voltammetry (CV). CV measurement was conducted using $K_3[Fe(CN)_6]$ as a conventional redox probe. The detection analyte was prepared using 30 mM $K_3[Fe(CN)_6]$ in 10 mM PBS. A fabricated SPCE was dipped in 5 mL of this buffer and CV analysis was conducted with -0.3V to 0.6V potential windows and 50 mV/s of scan rate.

2.5 Drop cast of MIP onto the WE of the SPE

MIP micro particles were dispersed in ethanol (1 mg/mL), drop cast (5 µL and 10 µL) onto the working electrode surface and allowed to dry at room temperature. The electrodes were thoroughly rinse with deionised water and the presence of MIPs on the surface was confirmed by CV analysis.

2.6 Electrochemical Analysis for Screening of SPCE Fabrication Parameters

Electrochemical analysis was performed to screen and compare the effects of fabrication parameters on SPCE performance. CV was employed as the primary screening technique using

https://doi.org/10.31436/iiumecp.v1i1.4443

a standard three-electrode configuration, with the fabricated SPCE as the working electrode, a carbon counter electrode, and an external Ag/AgCl reference electrode. A 30 mM potassium ferricyanide solution prepared in 10 mM phosphate-buffered saline (PBS) was used as a redox probe, and measurements were conducted within a potential window of −0.3 V to 0.6 V at a scan rate of 50 mV/s. The electrochemical responses of SPCEs fabricated using different carbon ink types, stencil fabrication methods, and MIP deposition volumes were systematically evaluated by comparing redox peak visibility, anodic and cathodic peak currents, peak-to-peak separation (ΔEp), and signal stability. Electrodes exhibiting lower ΔEp values, higher peak currents, and well-defined redox peaks were considered to demonstrate superior electron transfer efficiency and fabrication quality, allowing the identification of optimal fabrication parameters for subsequent sensor development.

3. RESULT & DISCUSSION

3.1 Synthesis of MIP and NIP

The MIP and NIP were synthesized based on method in Section 2.2 and were analyzed with SEM to evaluate their structural properties. The images in Figure 1 below show cluster shaped submicron particles. The leached-MIP (L-MIP), unleached-MIP (U-MIP) and NIP particles were found to be fairly similar in shape and size (U-MIP refers to the unleached MIP containing the SMX template prior to extraction, L-MIP denotes the leached MIP after removal of the SMX template to create specific binding cavities, and NIP represents the non-imprinted polymer synthesized without the SMX template). This is because all those polymers were synthesized using the same monomer and component that give them similar morphology and shape with the difference being SMX with binding site in U-MIP, binding site of the SMX in L-MIP, and no binding site in NIP.

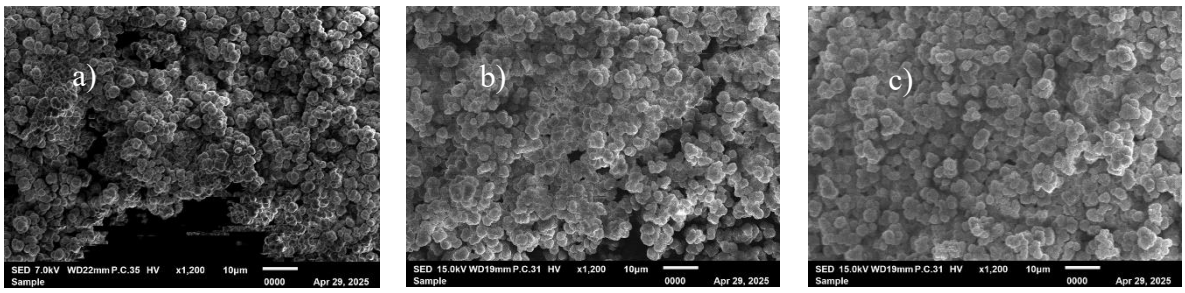

Figure 1: SEM analysis; (a) Unleached-MIP (U-MIP), (b) leached-MIP (L-MIP), (c) NIP

However, this cannot be seen in the images because the morphological changes induced by template extraction are often subtle and may not result in significant surface topography differences that are visually distinguishable under standard SEM imaging conditions and required FTIR to determine the SMX related peaks in polymers synthesized [13].

3.2 Screening of SPCE's Type of Carbon Ink

There are two different types of carbon ink that were used in the screening process to find the best type of ink to use in the MIP/SPCE which are carbon water-based ink and carbon solvent-based ink (C6-P1). Both inks can be used for SPE fabrication, but specific applications

https://doi.org/10.31436/iiumecp.v1i1.4443

need a specific ink type for SPE fabrication. Tests were conducted to assess several parameters, and the results are summarized in Table 1.

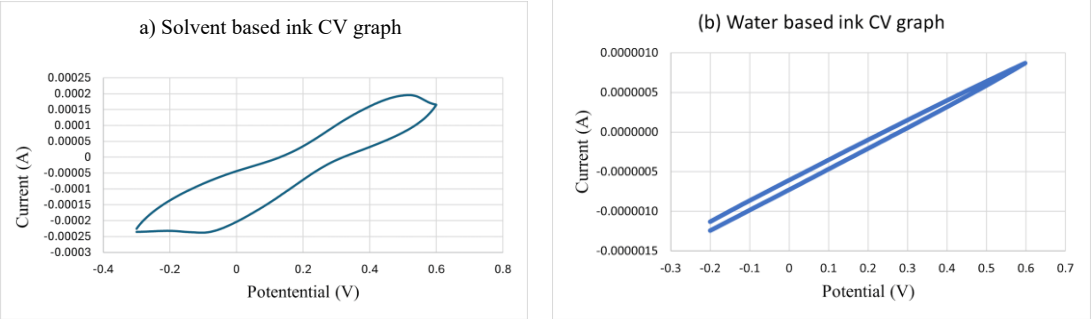

Figure 2: CV voltammogram at -0.3V to 0.6V and scan rate 50mV/s; (a) Solvent based carbon ink, (b) Water based carbon ink

Table 1: Comparison between water-based and solvent-based carbon ink

Types of Ink	Drying & Curing (Specification Sheet)	Redox Peak Visibility on Analysis Graph	SPCE Condition (During CV Test)	Resistance of the SPCE (Ω)
Water-based	D: 80°C for 5min C: 120°C for 20min	No	Tear off (surface become uneven)	~ 8000
Solvent-based	D: 80°C for 5min C: 140°C for 45min	Yes	Good Condition	200-400

CV analysis was performed for both carbon paste ink as shown in Figure 2, solvent-based carbon ink shows redox peak in CV analysis compared to water-based ink. The graph indicates that by using the water-based ink, there is no redox reaction occurring in the system and no electron transfer between buffer and working electrode, thus, causing no redox peak in CV analysis. The high resistance (8000 Ω) is the main reason for the disappearance of the peak as high resistance causes electron transfer harder between the electrode and buffer that prevent or severely limit the electron flow in the system. Therefore, solvent-based carbon ink is the best option for this application to detect and quantify SMX residue as it gave low resistance and reliability to make the system run smoothly without any disruption.

3.3 Screening of SPCE's Stencil Type

The technique used to fabricate SPCE in this research is called screen printing where it uses a stencil to print the carbon ink onto a PET sheet. There are two types of stencils used in this research to find the most reliable stencil to use in this research. Table 2 shows the result screen printed for two types of stencils used which are mesh stencil from Khai Lean Silk Screen Supplier Sdn Bhd and plotter cutter stencil produced by Silhouette Cameo V4 machine.

https://doi.org/10.31436/iiumecp.v1i1.4443

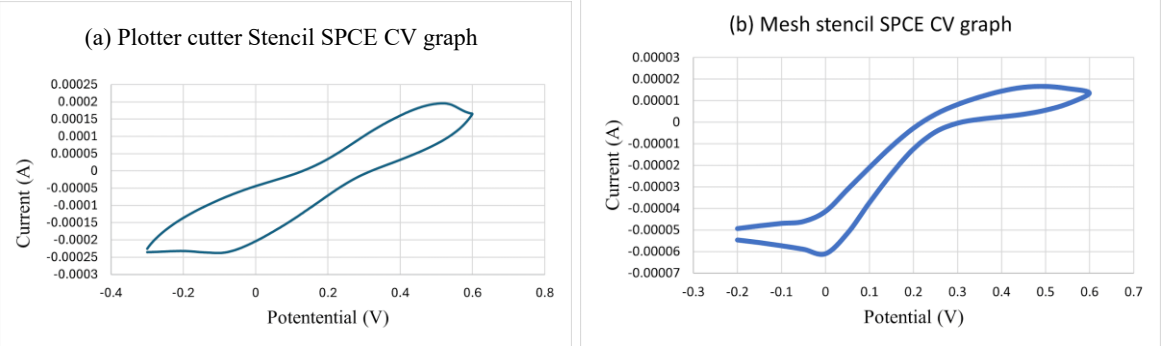

Figure 3: CV Voltammogram at -0.3V to 0.6V and scan rate 50mV/s; (a) Plotter cutter SPCE, (b) Mesh stencil SPCE

Table 2: Comparison between plotter cutter stencil & mesh stencil

Stencil Type	Resistance of SPCE (Ω)	Redox Peak Visibility
Plotter Cutter	200-400	Yes (higher peak: 2×10^{-4} A)
Mesh	6000	Almost no peak (low peak: 2×10^{-5} A)

The high resistance and almost no redox peak visibility indicates that by using the mesh stencil, there is no redox reaction occurring in the system and no electron transfer between buffer and working electrode, thus, causing no redox peak in CV analysis. The high resistance (6000 Ω) is the main reason for the disappearance of the peak as high resistance causes electron transfer harder between the electrode and buffer that prevent or severely limit the electron flow in the system.

Among the possible reasons that cause this issue is due to contaminated mesh. Contamination of the mesh stencil can occur due to residual ink from the previous printing process that obstruct the open areas of the mesh even after the cleaning process. The remaining ink on the mesh was difficult to be removed by the cleaning solvent as compared to the plotter cutter stencil. The material used could also be the reason for this problem, mesh stencil was made from nylon while plotter cutter stencil was made from PVC which is easier to remove the ink. When the mesh is clogged or dirty, Ink transfer becomes inconsistent, resulting in thinner or incomplete deposition on the substrate. This leads to poor electrical connectivity between carbon particles within the printed layer, increasing overall resistance. Furthermore, in severe cases, it can even cause breaks or gaps in the printed pattern, which can completely block electron flow and eliminate any redox peak in CV analysis [14]. Therefore, the plotter cutter stencil was identified as the more reliable fabrication approach for SPCE production, offering improved printing consistency, lower electrical resistance, and superior electrochemical performance for subsequent sensor development.

3.4 Screening of Deposition of MIP on working electrode of the SPCE

Once the screen-printing process was completed and the optimal SPCE fabrication parameters were established, the next critical step involved the modification of the working electrode surface with the MIP. To evaluate the effect of MIP deposition volume, the electrochemical responses of bare SPCE, 5 µL MIP-SPCE, and 10 µL MIP-SPCE were compared in Figure 4 and Table 3 below. There is some limitation while undergoing the deposition of the MIP as there was a screen printed SPCE that may have some irregular surface

https://doi.org/10.31436/iiumecp.v1i1.4443

that obstruct the process to deposit the MIP and cause the MIP solution always to leach out to counter electrode, thus only 5 µL and 10 µL of MIP were considered.

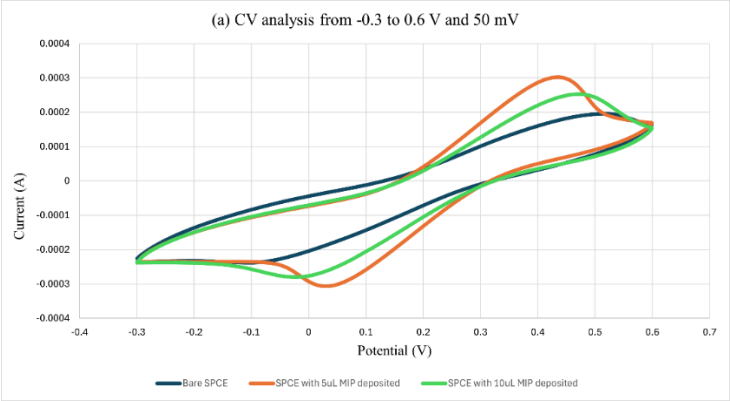

Figure 4: CV voltammogram in 30mM potassium ferricyanide in 10mM PBS at potential windows -0.3 to 0.6 V and 50 mV/s for bare, 5 µL and 10 µL MIP deposited SPCE

Table 3: Comparison between bare, 5 µL, and 10 µL MIP deposited SPCE.

SPCE Condition	Peak to peak separation, ΔEp (V)	Anodic peak current, Ip (A)
Bare SPCE	0.648	0.00021
5µL MIP deposited SPCE	0.395	0.00031
10µL MIP deposited SPCE	0.499	0.00025

Ultimately, these results emphasize the importance of MIP layer thickness. While thin films (5 µL) improve performance, excessive deposition (10 µL) may obstruct redox species transport and reduce sensitivity. Thus, 5 µL was found to be the optimal deposition volume for balancing electron transfer efficiency and analyte accessibility. Therefore, this deposition volume was selected as the optimized condition for subsequent sensor fabrication and electrochemical studies, ensuring reliable and reproducible SPCE performance.

4. CONCLUSION

This work emphasizes the importance of fabrication parameter screening in the design of a low-cost MIP-based electrochemical sensor for detecting SMX. The evaluation of key parameters revealed that solvent-based carbon ink produced SPCEs with significantly lower resistance and clearer redox behavior than water-based ink, whereas plotter cutter stencils produced more consistent electrode patterns and better electrochemical performance than mesh stencils. Screening of the MIP deposition volume yielded a 5 µL layer with the best balance of electron transfer efficiency and analyte accessibility, leading to higher anodic peak current compared to thicker coatings. These data suggest that carefully selecting the fabrication settings is critical for achieving consistent and reliable SPCE performance. The improved manufacturing configuration proposed in this study provides a solid foundation for future analytical validation and facilitates the creation of scalable, low-cost electrochemical sensors for routine antibiotic residue detection in food safety applications.

ACKNOWLEDGEMENT

This research was supported by FRGS-RACER Grant Scheme (RACER/1/2019/TK04/UIAM//2) from the Ministry of Higher Education, Malaysia.

REFERENCES

[1] Abdelgalil AA, Alkahtani HM, Al-Jenoobi FI. (2019) Profiles of Drug Substances, Excipients, and Related Methodology. Sorafenib, 44:239-266. https://doi.org/10.1016/bs.podrm.2018.11.003

[2] Sachi S, Ferdous J, Sikder M, Hussani S. (2019) Antibiotic residues in milk: Past, present, and future. Journal of Advanced Veterinary and Animal Research, 6(3):315. https://doi.org/10.5455/javar.2019.f350

[3] Sayari A, Alzyadi GA, Almudhihi TF, Aljabr SM. (2025) Determination of Antibiotic Residues in Milk Marketed in SaudiArabia and Their Dietary Risk Assessment. Journal of Food Science and Nutrition Research, 07-13. https://doi.org/10.26502/jfsnr.2642-110000171

[4] Shen Y, Sun Z, Zhao S, Chen F, Shi P, Zhao N, Sun K, Ye C, Lin C, Fu L. (2024) Screen-Printed Electrodes as Low-Cost Sensors for Breast Cancer Biomarker Detection. Sensors, 24(17):5679-5679. https://doi.org/10.3390/s24175679

[5] Simbine-Ribisse EO, Bila NM, Manhiça AJ, Macuamule CJ, Pavesi A. (2024) Antibiotic residues in dairy products in Africa: A systematic review. Food Chemistry Advances, 5:100822-100822. https://doi.org/10.1016/j.focha.2024.100822

[6] Virto M, Santamarina-García G, Amores G, Hernández I. (2022) Antibiotics in Dairy Production:Where Is the Problem? Dairy, 3(3):541-564. https://doi.org/10.3390/dairy3030039

[7] Mello GAB, Benjamin SR, de Lima F, Dutra RF. (2025) Recent Advances in Electrochemical Sensors for the Detection of Anti-Inflammatory and Antibiotic Drugs: A Comprehensive Review. Biosensors, 15(10):676. https://doi.org/10.3390/bios15100676

[8] Margaux F, Krupa MP, Hooyberghs, G Lowdon JW, Cleij TJ, Diliën H, Eersels K, Van Grinsven B. (2024) Electrochemical Sensors for Antibiotic Detection: A Focused Review with a Brief Overview of Commercial Technologies. Sensors, 24(17):5576-5576. https://doi.org/10.3390/s24175576

[9] Hatala M, Gemeiner P, Hvojnik M, Mikula M. (2018) The effect of the ink composition on the performance of carbon-based conductive screen printing inks. Journal of Materials Science: Materials in Electronics, 30(2):1034-1044. https://doi.org/10.1007/s10854-018-0372-7

[10] Supatinee K, Tubtimtong S, Thavarungkul P, Kanatharana P, Chang KH, Fahmi A, Limbut W. (2022) A Fabrication of Multichannel Graphite Electrode Using Low-Cost Stencil-Printing Technique. Sensors, 22(8):3034-3034. https://doi.org/10.3390/s22083034

[11] Bravo-Yagüe, JC, Paniagua-González G, Garcinuño RM, García-Mayor A, Fernández-Hernando P. (2025) Colorimetric Molecularly Imprinted Polymer-Based Sensors for Rapid Detection of Organic Compounds: A Review. Chemosensors, 13(5):163-163. https://doi.org/10.3390/chemosensors13050163

[12] Kadhem AJ, Gentile GJ, Fidalgo de Cortalezzi MM. (2021) Molecularly Imprinted Polymers (MIPs) in Sensors for Environmental and Biomedical Applications: A Review. Molecules, 26(20), 6233. https://doi.org/10.3390/molecules26206233

[13] Quinto KS, Vega-Chacón J, Mortari B, Wong A, Del M, Picasso G. (2023) Development and Characterization of a Molecularly Imprinted Polymer for the Selective Removal of Brilliant Green Textile Dye from River and Textile Industry Effluents. Polymers, 15(18):3709-3709. https://doi.org/10.3390/polym15183709

[14] Thibault C, Séverac C, Mingotaud AF, Vieu C, Mauzac M. (2007) Poly(dimethylsiloxane) Contamination in Microcontact Printing and Its Influence on Patterning Oligonucleotides. Langmuir, 23(21):10706-10714. https://doi.org/10.1021/la701841j